JACS
JOURNAL OF THE AMERICAN CHEMICAL SOCIETY
Article
Cite This: J. Am. Chem. Soc. 2018, 140, 15724−15730
pubs.acs.org/JACS

A Crystalline Polyimide Porous Organic Framework for Selective Adsorption of Acetylene over Ethylene

Lingchang Jiang,[†] Yuyang Tian,[‡] Tu Sun,[§] Youliang Zhu,[▽] Hao Ren,[†] Xiaoqin Zou,[‡] Yanhang Ma,*[,§] Katie R. Meihaus,[∥,⊥,#] Jeffrey R. Long,[∥,⊥,#] and Guangshan Zhu*[,†,‡]

[†]State Key Laboratory of Inorganic Synthesis and Preparative Chemistry, College of Chemistry, Jilin University, Changchun 130012, China

[‡]Key Laboratory of Polyoxometalate Science of the Ministry of Education, Faculty of Chemistry, Northeast Normal University, Changchun 130024, China

[§]School of Physical Science and Technology, ShanghaiTech University, Shanghai 201210, China

[▽]State Key Laboratory of Polymer Physics and Chemistry, Changchun Institute of Applied Chemistry, Chinese Academy of Sciences, Changchun 130022, China

[∥]Department of Chemistry, University of California, Berkeley, California 94720, United States

[⊥]Department of Chemical & Biomolecular Engineering, University of California, Berkeley, California 94720, United States

[#]Materials Sciences Division, Lawrence Berkeley National Laboratory, Berkeley, California 94720, United States

Supporting Information

ABSTRACT: The separation of acetylene from ethylene is a crucial process in the petrochemical industry, as even small acetylene impurities can lead to premature termination of ethylene polymerization. Herein, we present the synthesis of a robust, crystalline naphthalene diimide porous aromatic framework via imidization of linear naphthalene-1,4,5,8-tetracarboxylic dianhydride and triangular tris(4-aminophenyl)amine. The resulting material, PAF-110, exhibits impressive thermal and long-term structural stability, as indicated by thermogravimetric analysis and powder X-ray diffraction characterization. Gas adsorption characterization reveals that PAF-110 has a capacity for acetylene that is more than twice its ethylene capacity at 273 K and 1 bar, and it exhibits a moderate acetylene selectivity of 3.9 at 298 K and 1 bar. Complementary computational investigation of each guest binding in PAF-110 suggests that this affinity and selectivity for acetylene arises from its stronger electrostatic interaction with the carbonyl oxygen atoms of the framework. To the best of our knowledge, PAF-110 is the first crystalline porous organic material to exhibit selective adsorption of acetylene over ethylene, and its properties may provide insight into the further optimized design of porous organic materials for this key gas separation.

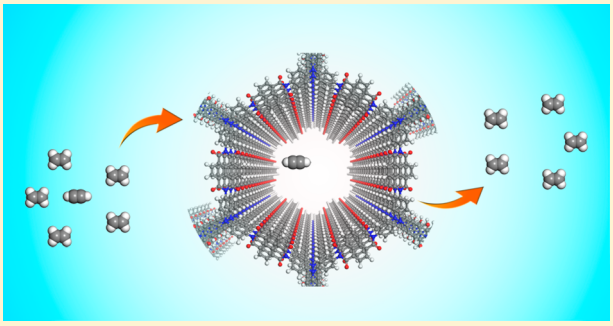

INTRODUCTION

Ethylene is a key commodity in the chemical, plastic, and agricultural industries and is produced globally on a massive scale—exceeding 150 million tons in 2015—primarily via hydrocarbon steam cracking.[1] A small amount of acetylene is generated as a byproduct of this process and is particularly detrimental to the downstream production of polyethylene, due to its role in early termination of catalysis.[2,3] Currently, the separation of acetylene from ethylene is carried out via cryogenic distillation, and acetylene may also be converted to ethylene via partial hydrogenation. Both of these processes are energy- and cost-intensive,[4] and therefore the development of a more energy-efficient means of carrying out the separation of acetylene from ethylene is of great interest and relevance to industry. Porous materials such as metal−organic frameworks have attracted tremendous attention for the separation of small molecules,[5] including hydrocarbons,[6] owing to their high structural tunability and the presence of metal centers that can polarize guests or strongly bind them at open coordination sites. Recently a few metal−organic frameworks have been discovered that are capable of the highly selective separation of acetylene from ethylene.[1,2,4]

Porous aromatic frameworks—also known as covalent organic frameworks or porous organic frameworks—are another emerging class of porous adsorbents[7−10] with demonstrated utility in gas separation,[11,12] catalysis,[13−16] photoconductivity,[17−20] proton conduction,[21] and many other applications.[7−10] These materials are extremely robust, owing to strong covalent bonds between organic building

Received: August 1, 2018
Published: October 26, 2018

DOI: 10.1021/jacs.8b08174
J. Am. Chem. Soc. 2018, 140, 15724−15730

units, and a wide variety of crystalline and amorphous variants have been discovered over the past decade.[11,22−35,38] Akin to their hybrid inorganic−organic metal−organic frameworks, these materials are also tunable, depending on the choice of organic building units,[7−13,22−24] and since their initial discovery,[34] crystalline porous organic materials have been obtained via a variety of routes, including through the use of boronic acid[35,36] or nitrile trimerizations,[29,37] imine formation,[38] and more recently imidizations.[39,40] While porous aromatic frameworks are of interest for a number of gas adsorption and separation applications,[7−12,22−24] only recently has one such material been designed and studied for the selective separation of acetylene from ethylene.[3]

Herein, we describe the synthesis and gas adsorption properties of a crystalline naphthalene diimide porous framework, PAF-110, prepared via an imidization reaction between naphthalene-1,4,5,8-tetracarboxylic dianhydride and tris(4-aminophenyl)amine. Notably, this material is highly robust and maintains crystallinity for at least one year in air, as well as in the presence of various coordinating solvents and acid. Additionally, this material exhibits a capacity for acetylene that is nearly twice that of ethylene and selective acetylene adsorption at ambient temperatures, and thus represents the first example of a crystalline porous organic framework capable of effecting this separation.

EXPERIMENTAL SECTION

General Procedures. Naphthalene-1,4,5,8-tetracarboxylic dianhydride (NTCDA) and tris(4-aminophenyl)amine (TAPA) were purchased from TCI (Shanghai) in 98% purity. Mesitylene, *N*-methyl-2-pyrrolidone (NMP), and isoquinoline were obtained from Aladdin Reagents in 97% purity. All chemicals were used as received.

Synthesis of PAF-110. A Pyrex tube (10 mm o.d., 8 mm i.d., 18 cm long) was charged with NTCDA (24.1 mg, 0.0899 mmol), TAPA (17.4 mg, 0.0599 mmol), mesitylene (0.65 mL), *N*-methyl-2-pyrrolidone (NMP) (0.3 mL), and isoquinoline (0.05 mL). The mixture was then flash frozen at 77 K using a liquid N_2 bath and degassed via three freeze−pump−thaw cycles. The tube was sealed under vacuum using a butane/O_2 flame and then heated at 160 °C for 5 days. After cooling to room temperature, filtration was used to collect the crude product as a dark brown precipitate. This powder was subsequently washed with tetrahydrofuran (THF) and then purified by Soxhlet extraction with THF (24 h) followed by methanol (24 h). The final activated PAF-110 material was obtained as a brown powder after drying under vacuum for 12 h at 120 °C (31.1 mg, 81.3% yield).

Instrumentation. Fourier Transform infrared spectroscopy measurements were performed on an IFS 66 V/S FT-IR spectrometer. Cross-polarization magic angle spinning ^{13}C NMR spectra were obtained using a Bruker AVANCE III 400 WB spectrometer. Thermogravimetric analysis data were collected in air using a Netzch Sta 449c thermal analyzer system using a heating rate of 10 °C/min. Scanning electron microscopy (SEM) images were conducted on JEOL JSM-6700 and JSM-7800F Prime instruments. Transmission electron microscopy (TEM) experiments were carried out on JEM-3010 and JEM-2100 Plus instruments. X-ray diffraction experiments were performed using a Rigaku D/MAX2550 diffractometer with Cu Kα radiation (1.541 Å) at 50 kV and 200 mA. Nitrogen adsorption isotherms were carried out at 77 K using a Quantachrome Autosorb iQ2 analyzer. Ultrahigh purity grade N_2, acetylene, and ethylene were used for all adsorption measurements. Where relevant, a liquid nitrogen bath was used to maintain a measurement temperature of 77 K.

RESULTS AND DISCUSSION

A number of amorphous, porous organic materials based on C4N and C5N imide rings have been previously reported and studied for various gas adsorption and separation applications.[41−45] However, only recently have there been reports of robust, crystalline, porous organic frameworks based on C4N imide rings.[39,40] We sought to synthesize a porous crystalline material built of C5N imide rings, as these are known to be even more stable than their five atom ring counterparts.[46,47] As shown in Figure 1a, the condensation of 1,8-naphthalic anhydride with aniline is one example of a reaction that could result in the formation of a C5N imide ring-containing product after the elimination of water. We thus sought to employ the symmetric naphthalene-1,4,5,8-tetracarboxylic dianhydride in constructing a C5N imide ring based porous framework. The reaction of NTCDA with D_3-symmetric tris(4-aminophenyl)amine in a mixture of mesitylene, *N*-methyl-2-pyrrolidone, and isoquinoline at 160 °C for 5 days resulted in a crude brown precipitate, PAF-110, that was further purified via Soxhlet extraction with THF and methanol. The material was found to be insoluble in common solvents such as water,

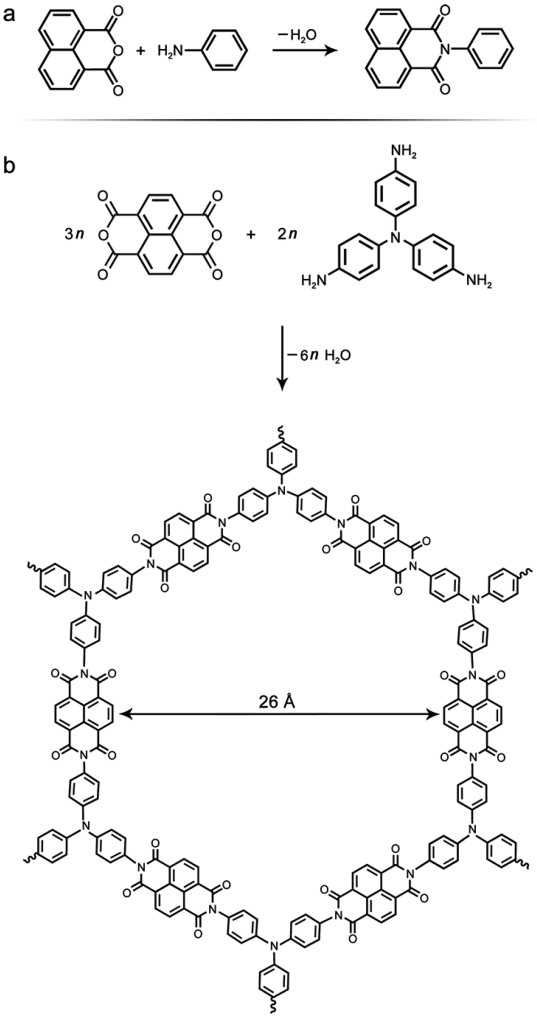

Figure 1. (a) Model reaction between 1,8-naphthalic anhydride and aniline to form a product containing a C5N imide ring. (b) Schematic representation of the synthesis of PAF-110 and proposed structure.

DOI: 10.1021/jacs.8b08174
J. Am. Chem. Soc. 2018, 140, 15724−15730

alkanes, alcohols, acetone, CH_2Cl_2, THF, methylbenzene, and *N*,*N*-dimethylformamide.

The proposed structure of PAF-110 is shown in Figure 1b, and successful imide bond formation was confirmed by Fourier transform infrared (FT-IR) spectroscopy and cross-polarization magic angle spinning (CP-MAS) ^{13}C NMR spectroscopy. In the IR spectrum of PAF-110 (Figure S1), characteristic absorption peaks for C═O (1673 cm^{-1}, 1716 cm^{-1}) and C−N−C groups (1344 cm^{-1}) indicated the successful formation of C5N six-membered imide rings, while the absence of characteristic peaks for NTCDA (C═O stretch at 1781 cm^{-1}) and TAPA (N−H stretch at 3336 cm^{-1}) confirmed that the imidization reaction went to completion. A CP-MAS ^{13}C NMR signal at 161.5 ppm was assigned to the carbonyl carbon of the six-membered imide ring of PAF-110, and several additional chemical shifts ranging from 110 to 150 ppm were assigned to phenyl carbon atoms (Figure S2). Thermogravimetric analysis further revealed that PAF-110 possesses high thermal stability up to 530 °C (Figure S3) and is among the most thermally stable crystalline organic frameworks reported to date.

The morphology and size of the as-synthesized PAF-110 particles were characterized using SEM. As shown in Figure 2a, the material forms small, highly aggregated particles, ranging in size from 20 to 100 nm. TEM was also used to investigate the structure of PAF-110 (Figure 2b−d). Clear lattice fringes with coherence lengths on the order of 10 nm were commonly observed in many small domains (Figure 2b). Contiguous straight channels with a spacing of 2.6 nm could also be detected (Figure 2c), and several domains viewed from another orientation show a hexagonal pore arrangement (Figure 2d). However, we did not observe electron diffraction spots in the selected area of the electron diffraction pattern, likely due to small crystallite sizes, the weak scattering power of carbon and nitrogen, and a strong background (see Figures S4 and S5).

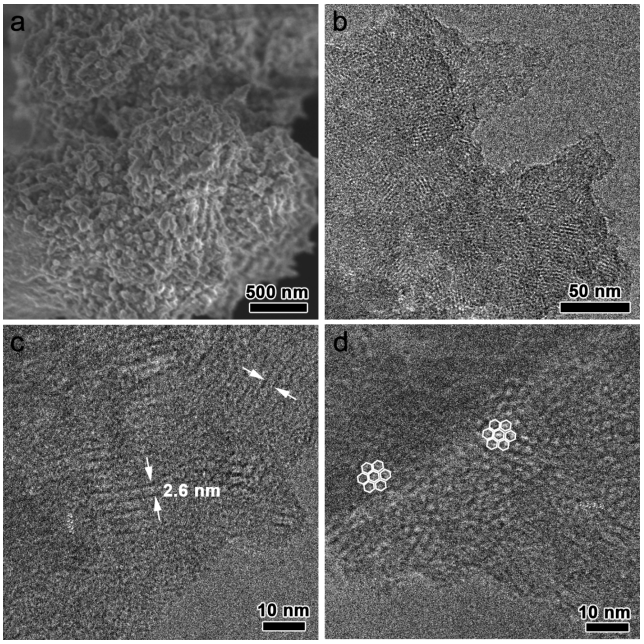

Figure 2. SEM image (a) and TEM images (b−d) of PAF-110. The white arrows in (c) highlight the straight channels with a diameter of ~2.6 nm, and the hexagonal pores are highlighted in (d).

Based on this extended local structure information from TEM results, a hexagonal crystal structure was proposed for PAF-110. Given the nature of the bonding between the NTCDA and TAPA building units, their assembly into a two-dimensional hexagonal layer should be more or less fixed, while packing along the perpendicular direction remains variable. We considered the two extreme cases of eclipsed (AA) and staggered (AB) stacking models[33,34,48−50] in Materials Studio (Figure 3, inset) and calculated their powder patterns (Figure 3, blue and purple traces, respectively). After comparing with the experimental powder X-ray diffraction pattern for PAF-110 at room temperature (Figure 3, black trace), the AA stacking model was deemed optimal, and Pawley refinement accordingly yielded the following unit cell parameters: $a = b = 32.18$ Å, $c = 4.37$ Å, $\alpha = \beta = 90°$, $\gamma = 120°$ with good residual factors of $R_{wp} = 3.35\%$ and $R_p = 2.62\%$ (Figure 3, red trace). Peaks at 3.10°, 6.43°, 8.48°, and 20.72° were indexed as 100, 200, 210, and 001 reflections, respectively.

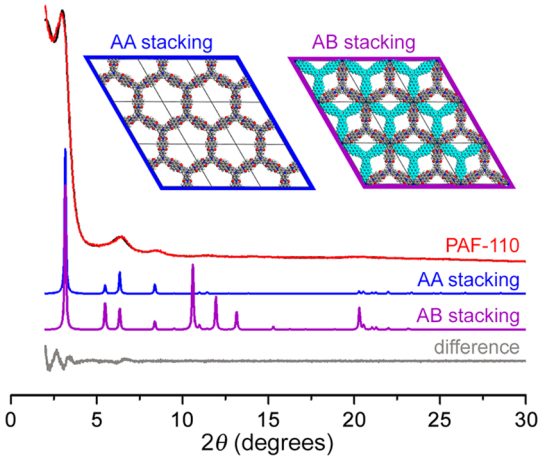

Figure 3. Experimental (black), refined (red), simulated AA stacking (blue), simulated AB stacking (purple), and difference (gray) powder X-ray diffraction patterns for PAF-110; (inset) illustration of the AA and AB stacking models for PAF-110. Cu Kα radiation was used.

Nitrogen adsorption data collected for PAF-110 at 77 K indicated the material is permanently porous (Figure 4a), with a Brunauer−Emmett−Teller (BET) surface area of 910 m^2/g. It is worth noting that this surface area is significantly higher than amorphous, porous NPI-2 (SA_{BET} = 291 m^2/g),[51] although both materials are prepared from the same precursor molecules. The total pore volume of PAF-110 was also estimated from the isotherm data to be 0.59 cm^3/g (P/P_0 = 0.9), and the pore size distribution was modeled using quenched solid state functional theory, utilizing the model N_2 on carbon at 77 K (Figure 4b). The main pore sizes of PAF-110 were found to be centered at 17 and 25 Å. While the latter size agrees well with the theoretical 26 Å pore for the simulated structure, the AA stacking model does not account for a 17 Å aperture. One possible explanation for the observed distribution is the existence of a smaller, secondary pore cavity that is also accessible to guests. A recent study of anionic silicate organic frameworks constructed from 9,10-dimethyl-2,3,6,7-tetrahydroxyanthracene also found a bimodal pore size distribution, which the authors attributed to sequential filling of small and main pore cavities. The smaller cavities were

DOI: 10.1021/jacs.8b08174
J. Am. Chem. Soc. 2018, 140, 15724−15730

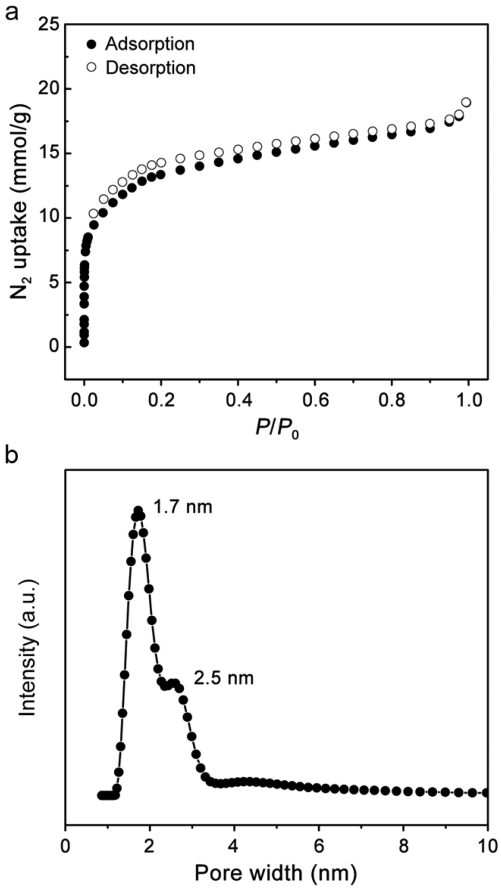

Figure 4. (a) Nitrogen isotherms and (b) the pore size distribution for PAF-110.

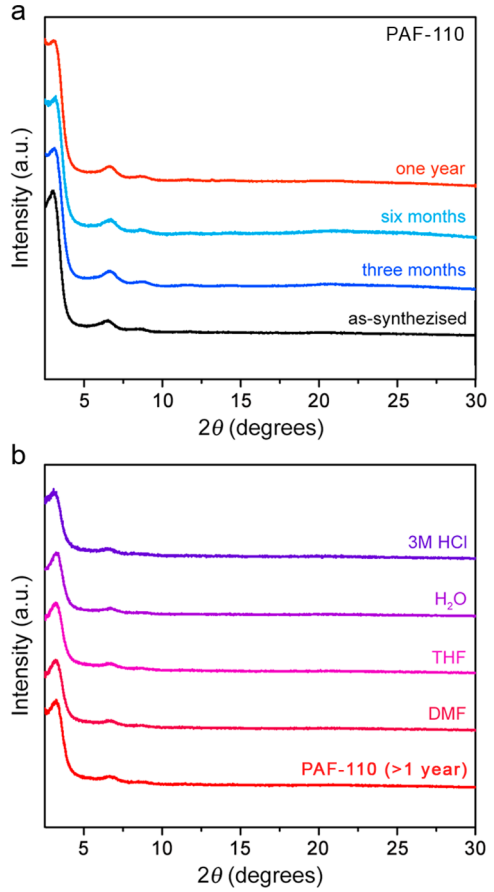

Figure 5. (a) Powder X-ray diffraction patterns for PAF-110 as-synthesized and after air exposure for three months, six months, and one year. (b) Powder X-ray diffraction patterns for a sample of PAF-110 stored in air >1 year following treatment with various solvents and acid; samples were treated by soaking in a given solvent for 7 days at room temperature.

identified near the methyl-functionalized anthracene rings from modeling of solvent-accessible voids.[52] We believe that a similar two-step filling process might be occurring in PAF-110.

At a minimum, porous adsorbents should exhibit long-term stability in air to be viable for application in an industrial separation. The robustness of PAF-110 was first monitored by collecting its powder X-ray diffraction pattern after exposure to air under ambient conditions for varying lengths of time, ranging from immediately after synthesis to one year (Figure 5a). The diffraction data indicate that PAF-110 is stable for at least one year without significant structural degradation. To the best of our knowledge, this is the longest period of time under which a porous aromatic framework has been shown to maintain its crystallinity. A sample of PAF-110 exposed to air for more than one year also retained its crystallinity following treatment with different solvents and even 3 M aqueous HCl (Figure 5b).

Acetylene and ethylene adsorption isotherms were measured at 273, 298, and 308 K (see Figure 6 and Figures S8 and S9). At 273 K and 1 bar, PAF-110 exhibits an acetylene capacity of 3.48 mmol/g, which is more than double that for ethylene (1.61 mmol/g) under the same conditions, a result that suggests the potential of this material for acetylene/ethylene separations at near-ambient conditions. At room temperature and 1 bar, the framework adsorption capacity for each gas decreases, although the capacity for acetylene is still nearly twice that of ethylene (2.23 and 1.29 mmol/g, respectively). The isosteric heats of adsorption (Q_{st}) for each gas were estimated using the Clausius–Clapeyron equation following fitting of the isotherm data using the dual-site Langmuir–Freundlich model (Figures S10 and S11).[53,54] At close to zero loading, the Q_{st} values for acetylene and ethylene are −38.4 and −22.6 kJ/mol, respectively, indicating that PAF-110 has a greater affinity for acetylene at this temperature.

In order to shed light on this behavior, calculations of guest binding in PAF-110 were carried out using the Dmol3 module in Materials Studio. The calculations predicted that guest binding occurs primarily via electrostatic interactions between acetylene or ethylene hydrogen atoms and the carbonyl oxygen atoms of PAF-110, with associated binding energies of −22.8 and −16.1 kJ/mol, respectively (Figure 7). Interestingly, acetylene is also predicted to bind much more closely to the framework oxygen than ethylene, at a distance of 2.90 vs 3.14 Å. These computational results suggest that PAF-110 has a stronger electrostatic interaction with acetylene than ethylene and are consistent with the adsorption data and calculated Q_{st} values. The equimolar acetylene/ethylene adsorption selectivity of PAF-110 was also calculated using ideal adsorbed solution theory[55] (IAST) (Figure 6c). The calculated selectivities range from 3.9 to 8.0 at 298 K, exceeding the selectivities of the only other porous organic polymer reported for this separation, namely, CTF-PO71 (1.8 to 2.8).[3] We additionally collected adsorption isotherms using a sample of PAF-110 exposed to air for more than one year (Figure S17),

DOI: 10.1021/jacs.8b08174
J. Am. Chem. Soc. 2018, 140, 15724–15730

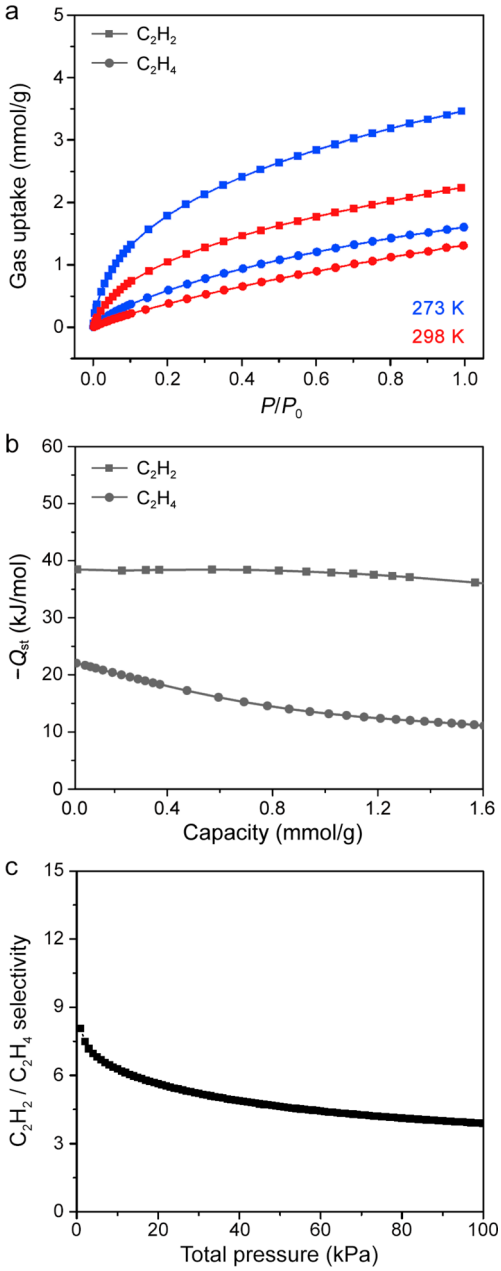

Figure 6. (a) Acetylene (squares) and ethylene (circles) adsorption isotherms for PAF-110 at 273 K (blue symbols) and 298 K (red symbols). P_0 = 1 bar. (b) Isosteric heats of adsorption, Q_{st}, for acetylene and ethylene. (c) Acetylene/ethylene adsorption selectivity of PAF-110 at 298 K, as determined from ideal adsorbed solution theory.

and from these data calculated IAST selectivity values (Figure S18). Notably, the results reveal similar acetylene and ethylene capacities and selectivity values to those obtained on a freshly prepared sample of the framework. Breakthrough experiments carried out using a freshly prepared PAF-110 sample further revealed that the equimolar acetylene/ethylene adsorption selectivity of PAF-110 is 4.5(±0.3) at 298 K and 1 bar (Figure S19), a value that is in good agreement with the predicted IAST value (3.9). Over all pressures, the selectivity of PAF-110 also surpasses that of some metal−organic frameworks, such as Fe_2(dobdc) (Fe-MOF-74, selectivity = 1.87; $dobdc^{4-}$ = 2,5-dioxido-1,4-benzenedicarboxylate),[56] the mixed-metal material

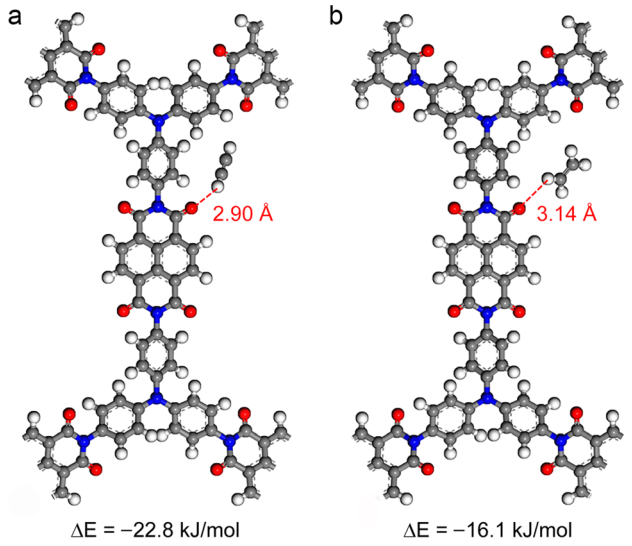

Figure 7. Optimized binding sites and binding energies for (a) acetylene and (b) ethylene within PAF-110.

$Zn_3(BDC)_3[Cu(SalPyCy)]$ (M′MOF-2a, selectivity = 1.93; BDC^{2-} = 1,4-benzenedicarboxylate, SalPyCy = salen-based ligand),[57] and $[Al_2(OH)_2(L)]$ (NOTT-300, selectivity = 2.3; L^{4-} = biphenyl-3,3′,5,5′-tetracarboxylate),[58] but is superseded by the selectivities of frameworks such as the interpenetrated material $[Cu(dpa)_2(SIF_6)]$ (SIFSIX-2-Cu-i, selectivity = 41.01; 4,4′-dipyridylacetylene)[1] and $[Zn(dps)_2(SiF_6)]$ (UTSA-300a, selectivity > 10^4; dps = 4,4′-dipyridylsulfide).[59]

CONCLUSIONS

In summary, a new crystalline porous aromatic framework, PAF-110, containing C5N imide rings has been successfully synthesized from naphthalene-1,4,5,8-tetracarboxylic dianhydride and tris(4-aminophenyl)amine. This material is the first example of a crystalline porous organic framework capable of selective separation of acetylene from ethylene, and it notably shows significant thermal and long-term stability that is advantageous for practical applications. At 298 K and 1 bar, the acetylene capacity of PAF-110 is nearly double that for ethylene, and the framework exhibits a moderate acetylene/ethylene selectivity of 3.9 under the same conditions. Calculations suggest that these properties stem in part from a stronger electrostatic interaction between PAF-110 and acetylene, which is mediated via close hydrogen bonding between the carbonyl oxygen atoms of the framework and the hydrogen atoms of acetylene.

ASSOCIATED CONTENT

Supporting Information

The Supporting Information is available free of charge at The Supporting Information is available free of charge on the ACS Publications website at DOI: 10.1021/jacs.8b08174.

FT-IR spectra, ^{13}C NMR spectra, TGA data, additional SEM and TEM images, calculated selectivity from IAST and breakthrough experiments (PDF)

AUTHOR INFORMATION

Corresponding Authors

*mayh2@shanghaitech.edu.cn
*zhugs@jlu.edu.cn

DOI: 10.1021/jacs.8b08174
J. Am. Chem. Soc. 2018, 140, 15724−15730

ORCID
Xiaoqin Zou: 0000-0002-8401-5538
Jeffrey R. Long: 0000-0002-5324-1321
Guangshan Zhu: 0000-0002-5794-3822

Notes

The authors declare no competing financial interest.

■ ACKNOWLEDGMENTS

We acknowledge funding support from National Basic Research Program of China (973 Program, grant no. 2014CB931804), National Science Foundation of China (NSFC grant nos. 21531003, 21501024, 91622106, 21875140), Major International (Regional) Joint Research Project of NSFC (grant no. 21120102034), the Commission for Science and Technology of Shanghai Municipality (17ZR1418600), and the Young Elite Scientist Sponsorship Program by CAST (2017QNRC001). Y.M. thanks Prof. Osamu Terasaki (ShanghaiTech University, China) for discussions. The contributions of K.R.M. and J.R.L. were supported through the Center for Gas Separations, an Energy Frontier Research Center funded by the U.S. Department of Energy, Office of Science, Office of Basic Energy Sciences, under Award DE-SC0001015.

■ REFERENCES

(1) Cui, X. L.; Chen, K. J.; Xing, H. B.; Yang, Q. W.; Krishna, R.; Bao, Z. B.; Wu, H.; Zhou, W.; Dong, X. L.; Han, Y.; Li, B.; Ren, Q. L.; Zaworotko, M. J.; Chen, B. L. Pore chemistry and size control in hybrid porous materials for acetylene capture from ethylene. *Science* **2016**, *353*, 141−144.

(2) Wen, H. M.; Li, B.; Wang, H. L.; Krishna, R.; Chen, B. L. High acetylene/ethylene separation in a microporous zinc(II) metal-organic framework with low binding energy. *Chem. Commun.* **2016**, *52*, 1166−1169.

(3) Lu, Y.; He, J.; Chen, Y. L.; Wang, H.; Zhao, Y. F.; Han, Y.; Ding, Y. Effective Acetylene/Ethylene Separation at Ambient Conditions by a Pigment-Based Covalent-Triazine Framework. *Macromol. Rapid Commun.* **2018**, *39*, 1700468.

(4) (a) Lee, J.; Chuah, C. Y.; Kim, J.; Kim, Y.; Ko, N.; Seo, Y. Y.; Kim, K.; Bae, T. H.; Lee, E. Separation of Acetylene from Carbon Dioxide and Ethylene by a Water-Stable Microporous Metal-Organic Framework with Aligned Imidazolium Groups inside the Channels. *Angew. Chem., Int. Ed.* **2018**, *57*, 7869−7873. (b) Hazra, A.; Jana, S.; Bonakala, S.; Balasubramanian, S.; Maji, T. K. Separation/purification of ethylene from an acetylene/ethylene mixture in a pillared-layer porous metal-organic framework. *Chem. Commun.* **2017**, *53*, 4907−4910.

(5) Li, H.; Wang, K. C.; Sun, Y. J.; Lollar, C. T.; Li, J. L.; Zhou, H. C. Recent advances in gas storage and separation using metal-organic frameworks. *Mater. Today* **2018**, *21*, 108−121.

(6) (a) Bao, Z. B.; Chang, G. G.; Xing, H. B.; Krishna, R.; Ren, Q. L.; Chen, B. L. Potential of microporous metal-organic frameworks for separation of hydrocarbon mixtures. *Energy Environ. Sci.* **2016**, *9*, 3612−3641. (b) Herm, Z. R.; Bloch, E. D.; Long, J. R. Hydrocarbon Separations in Metal-Organic Frameworks. *Chem. Mater.* **2014**, *26*, 323−338.

(7) (a) Van Humbeck, J. F.; Aubrey, M. L.; Alsbaiee, A.; Ameloot, R.; Coates, G. W.; Dichtel, W. R.; Long, J. R. Tetraarylborate Polymer Networks as Single-Ion Conducting Solid Electrolytes. *Chem. Sci.* **2015**, *6*, 5499−5505. (b) McKeown, N. B.; Budd, P. M. Exploitation of Intrinsic Microporosity in Polymer-Based Materials. *Macromolecules* **2010**, *43*, 5163−5176.

(8) Dawson, R.; Cooper, A. I.; Adams, D. J. Nanoporous organic polymer networks. *Prog. Polym. Sci.* **2012**, *37*, 530−563.

(9) Zou, X. Q.; Ren, H.; Zhu, G. S. Topology-directed design of porous organic frameworks and their advanced applications. *Chem. Commun.* **2013**, *49*, 3925−3936.

(10) Ding, S. Y.; Wang, W. Covalent organic frameworks (COFs): from design to applications. *Chem. Soc. Rev.* **2013**, *42*, 548−568.

(11) Furukawa, H.; Yaghi, O. M. Storage of Hydrogen, Methane, and Carbon Dioxide in Highly Porous Covalent Organic Frameworks for Clean Energy Applications. *J. Am. Chem. Soc.* **2009**, *131*, 8875−8883.

(12) (a) Han, S. S.; Mendoza-Cortes, J. L.; Goddard, W. A. Recent advances on simulation and theory of hydrogen storage in metal-organic frameworks and covalent organic frameworks. *Chem. Soc. Rev.* **2009**, *38*, 1460−1476. (b) Van Humbeck, J. F.; McDonald, T. M.; Jing, X.; Wiers, B. M.; Zhu, G.; Long, J. R. Ammonia Capture in Porous Organic Polymers Densely Functionalized with Brønsted Acid Groups. *J. Am. Chem. Soc.* **2014**, *136*, 2432−2440.

(13) Ding, S. Y.; Gao, J.; Wang, Q.; Zhang, Y.; Song, W. G.; Su, C. Y.; Wang, W. Construction of Covalent Organic Framework for Catalysis: Pd/COF-LZU1 in Suzuki-Miyaura Coupling Reaction. *J. Am. Chem. Soc.* **2011**, *133*, 19816−19822.

(14) Lin, S.; Diercks, C. S.; Zhang, Y. B.; Kornienko, N.; Nichols, E. M.; Zhao, Y. B.; Paris, A. R.; Kim, D.; Yang, P.; Yaghi, O. M.; Chang, C. J. Covalent organic frameworks comprising cobalt porphyrins for catalytic CO_2 reduction in water. *Science* **2015**, *349*, 1208−1213.

(15) Stegbauer, L.; Schwinghammer, K.; Lotsch, B. V. A hydrazone-based covalent organic framework for photocatalytic hydrogen production. *Chem. Sci.* **2014**, *5*, 2789−2793.

(16) Fang, Q. R.; Gu, S.; Zheng, J.; Zhuang, Z. B.; Qiu, S. L.; Yan, Y. S. 3D Microporous Base-Functionalized Covalent Organic Frameworks for Size-Selective Catalysis. *Angew. Chem., Int. Ed.* **2014**, *53*, 2878−2882.

(17) Wan, S.; Guo, J.; Kim, J.; Ihee, H.; Jiang, D. L. A Belt-Shaped, Blue Luminescent, and Semiconducting Covalent Organic Framework. *Angew. Chem., Int. Ed.* **2008**, *47*, 8826−8830.

(18) Colson, J. W.; Woll, A. R.; Mukherjee, A.; Levendorf, M. P.; Spitler, E. L.; Shields, V. B.; Spencer, M. G.; Park, J.; Dichtel, W. R. Oriented 2D Covalent Organic Framework Thin Films on Single-Layer Graphene. *Science* **2011**, *332*, 228−231.

(19) Dogru, M.; Handloser, M.; Auras, F.; Kunz, T.; Medina, D.; Hartschuh, A.; Knochel, P.; Bein, T. A Photoconductive Thienothiophene-Based Covalent Organic Framework Showing Charge Transfer Towards Included Fullerene. *Angew. Chem., Int. Ed.* **2013**, *52*, 2920−2924.

(20) Calik, M.; Auras, F.; Salonen, L. M.; Bader, K.; Grill, I.; Handloser, M.; Medina, D. D.; Dogru, M.; Lobermann, F.; Trauner, D.; Hartschuh, A.; Bein, T. Extraction of Photogenerated Electrons and Holes from a Covalent Organic Framework Integrated Heterojunction. *J. Am. Chem. Soc.* **2014**, *136*, 17802−17807.

(21) Ma, H. P.; Liu, B. L.; Li, B.; Zhang, L. M.; Li, Y. G.; Tan, H. Q.; Zang, H. Y.; Zhu, G. S. Cationic Covalent Organic Frameworks: A Simple Platform of Anionic Exchange for Porosity Tuning and Proton Conduction. *J. Am. Chem. Soc.* **2016**, *138*, 5897−5903.

(22) Jiang, J. X.; Su, F.; Trewin, A.; Wood, C. D.; Campbell, N. L.; Niu, H.; Dickinson, C.; Ganin, A. Y.; Rosseinsky, M. J.; Khimyak, Y. Z.; Cooper, A. I. Conjugated microporous poly (aryleneethynylene) networks. *Angew. Chem., Int. Ed.* **2007**, *46*, 8574−8578.

(23) Jiang, J. X.; Su, F.; Trewin, A.; Wood, C. D.; Niu, H.; Jones, J. T. A.; Khimyak, Y. Z.; Cooper, A. I. Synthetic control of the pore dimension and surface area in conjugated microporous polymer and copolymer networks. *J. Am. Chem. Soc.* **2008**, *130*, 7710−7720.

(24) Cooper, A. I. Conjugated Microporous Polymers. *Adv. Mater.* **2009**, *21*, 1291−1295.

(25) Dawson, R.; Laybourn, A.; Khimyak, Y. Z.; Adams, D. J.; Cooper, A. I. High Surface Area Conjugated Microporous Polymers: The Importance of Reaction Solvent Choice. *Macromolecules* **2010**, *43*, 8524−8530.

(26) McKeown, N. B.; Budd, P. M.; Msayib, K. J.; Ghanem, B. S.; Kingston, H. J.; Tattershall, C. E.; Makhseed, S.; Reynolds, K. J.; Fritsch, D. Polymers of Intrinsic Microporosity (PIMs): Bridging the

DOI: 10.1021/jacs.8b08174
J. Am. Chem. Soc. 2018, 140, 15724−15730

Void between Microporous and Polymeric Materials. *Chem. - Eur. J.* **2005**, *11*, 2610−2620.
(27) Carta, M.; Malpass-Evans, R.; Croad, M.; Rogan, Y.; Jansen, J. C.; Bernardo, P.; Bazzarelli, F.; McKeown, N. B. An Efficient Polymer Molecular Sieve for Membrane Gas Separations. *Science* **2013**, *339*, 303−307.
(28) Kuhn, P.; Antonietti, M.; Thomas, A. Porous, covalent triazine-based frameworks prepared by ionothermal synthesis. *Angew. Chem., Int. Ed.* **2008**, *47*, 3450−3453.
(29) Ren, S. J.; Bojdys, M. J.; Dawson, R.; Laybourn, A.; Khimyak, Y. Z.; Adams, D. J.; Cooper, A. I. Porous, Fluorescent, Covalent Triazine-Based Frameworks Via Room-Temperature and Microwave-Assisted Synthesis. *Adv. Mater.* **2012**, *24*, 2357−2361.
(30) Ben, T.; Ren, H.; Ma, S. Q.; Cao, D. P.; Lan, J. H.; Jing, X. F.; Wang, W. C.; Xu, J.; Deng, F.; Simmons, J. M.; Qiu, S. L.; Zhu, G. S. Targeted Synthesis of a Porous Aromatic Framework with High Stability and Exceptionally High Surface Area. *Angew. Chem., Int. Ed.* **2009**, *48*, 9457−9460.
(31) Ren, H.; Ben, T.; Wang, E. S.; Jing, X. F.; Xue, M.; Liu, B. B.; Cui, Y.; Qiu, S. L.; Zhu, G. S. Targeted synthesis of a 3D porous aromatic framework for selective sorption of benzene. *Chem. Commun.* **2010**, *46*, 291−293.
(32) Ren, H.; Ben, T.; Sun, F. X.; Guo, M. Y.; Jing, X. F.; Ma, H. P.; Cai, K.; Qiu, S. L.; Zhu, G. S. Synthesis of a porous aromatic framework for adsorbing organic pollutants application. *J. Mater. Chem.* **2011**, *21*, 10348−10353.
(33) Diercks, C. S.; Yaghi, O. M. The atom, the molecule, and the covalent organic framework. *Science* **2017**, *355*, 923−931.
(34) Cote, A. P.; Benin, A. I.; Ockwig, N. W.; O'Keeffe, M.; Matzger, A. J.; Yaghi, O. M. Porous, Crystalline, Covalent Organic Frameworks. *Science* **2005**, *310*, 1166−1170.
(35) El-Kaderi, H. M.; Hunt, J. R.; Mendoza-Cortes, J. L.; Cote, A. P.; Taylor, R. E.; O'Keeffe, M.; Yaghi, O. M. Designed synthesis of 3D covalent organic frameworks. *Science* **2007**, *316*, 268−272.
(36) Wan, S.; Guo, J.; Kim, J.; Ihee, H.; Jiang, D. L. A Photoconductive Covalent Organic Framework: Self-Condensed Arene Cubes Composed of Eclipsed 2D Polypyrene Sheets for Photocurrent Generation. *Angew. Chem., Int. Ed.* **2009**, *48*, 5439−5442.
(37) Bojdys, M. J.; Jeromenok, J.; Thomas, A.; Antonietti, M. Rational Extension of the Family of Layered, Covalent, Triazine-Based Frameworks with Regular Porosity. *Adv. Mater.* **2010**, *22*, 2202−2205.
(38) Uribe-Romo, F. J.; Hunt, J. R.; Furukawa, H.; Klock, C.; O'Keeffe, M.; Yaghi, O. M. A Crystalline Imine-Linked 3-D Porous Covalent Organic Framework. *J. Am. Chem. Soc.* **2009**, *131*, 4570−4571.
(39) Fang, Q. R.; Wang, J. H.; Gu, S.; Kaspar, R. B.; Zhuang, Z. B.; Zheng, J.; Guo, H. X.; Qiu, S. L.; Yan, Y. S. 3D Porous Crystalline Polyimide Covalent Organic Frameworks for Drug Delivery. *J. Am. Chem. Soc.* **2015**, *137*, 8352−8355.
(40) Fang, Q. R.; Zhuang, Z. B.; Gu, S.; Kaspar, R. B.; Zheng, J.; Wang, J. H.; Qiu, S. L.; Yan, Y. S. Designed synthesis of large-pore crystalline polyimide covalent organic frameworks. *Nat. Commun.* **2014**, *5*, 4503−4510.
(41) Weber, J.; Antonietti, M.; Thomas, A. Microporous networks of high-performance polymers: Elastic deformations and gas sorption properties. *Macromolecules* **2008**, *41*, 2880−2885.
(42) Wang, Z. G.; Zhang, B. F.; Yu, H.; Sun, L. X.; Jiao, C. L.; Liu, W. S. Microporous polyimide networks with large surface areas and their hydrogen storage properties. *Chem. Commun.* **2010**, *46*, 7730−7732.
(43) Farha, O. K.; Bae, Y. S.; Hauser, B. G.; Spokoyny, A. M.; Snurr, R. Q.; Mirkin, C. A.; Hupp, J. T. Chemical reduction of a diimide based porous polymer for selective uptake of carbon dioxide versus methane. *Chem. Commun.* **2010**, *46*, 1056−1058.
(44) Wang, Z. G.; Zhang, B. F.; Yu, H.; Li, G. Y.; Bao, Y. J. Synthetic control of network topology and pore structure in microporous polyimides based on triangular triphenylbenzene and triphenylamine units. *Soft Matter* **2011**, *7*, 5723−5730.
(45) Yang, Y. Q.; Zhang, Q.; Zhang, Z. G.; Zhang, S. B. Functional microporous polyimides based on sulfonated binaphthalene dianhydride for uptake and separation of carbon dioxide and vapors. *J. Mater. Chem. A* **2013**, *1*, 10368−10374.
(46) Rusanov, A. L. Novel Bis(Naphthalic Anhydrides) and Their Polyheteroarylenes with Improved Processability. *Adv. Polym. Sci.* **1994**, *111*, 115−175.
(47) Lee, C.; Sundar, S.; Kwon, J.; Han, H. Structure−Property Correlations of Sulfonated Polyimides. II. Effect of Substituent Groups on Membrane Properties. *J. Polym. Sci., Part A: Polym. Chem.* **2004**, *42*, 3621−3630.
(48) Cote, A. P.; El-Kaderi, H. M.; Furukawa, H.; Hunt, J. R.; Yaghi, O. M. Reticular synthesis of microporous and mesoporous 2D covalent organic frameworks. *J. Am. Chem. Soc.* **2007**, *129*, 12914−12915.
(49) Jin, E. Q.; Asada, M.; Xu, Q.; Dalapati, S.; Addicoat, M. A.; Brady, M. A.; Xu, H.; Toshikazu Nakamura, T.; Heine, T.; Chen, Q. H.; Jiang, D. L. Two-dimensional sp2 carbon−conjugated covalent organic frameworks. *Science* **2017**, *357*, 673−676.
(50) Feng, X.; Ding, X. S.; Jiang, D. L. Covalent organic frameworks. *Chem. Soc. Rev.* **2012**, *41*, 6010−6022.
(51) Li, G. Y.; Wang, Z. G. Naphthalene-Based Microporous Polyimides: Adsorption Behavior of CO2 and Toxic Organic Vapors and Their Separation from Other Gases. *J. Phys. Chem. C* **2013**, *117*, 24428−24437.
(52) Roeser, J.; Prill, D.; Bojdys, M. J.; Fayon, P.; Trewin, A.; Fitch, A. N.; Schmidt, M. U.; Thomas, A. Anionic silicate organic frameworks constructed from hexacoordinate silicon centres. *Nat. Chem.* **2017**, *9*, 977−982.
(53) Li, B. Y.; Zhang, Y. M.; Krishna, R.; Yao, K. X.; Han, Y.; Wu, Z. L.; Ma, D. X.; Shi, Z.; Pham, T.; Space, B.; Liu, J.; Thallapally, P. K.; Liu, J.; Chrzanowski, M.; Ma, S. Q. Introduction of pi-Complexation into Porous Aromatic Framework for Highly Selective Adsorption of Ethylene over Ethane. *J. Am. Chem. Soc.* **2014**, *136*, 8654−8660.
(54) He, Y. B.; Krishna, R.; Chen, B. L. Metal-organic frameworks with potential for energy-efficient adsorptive separation of light hydrocarbons. *Energy Environ. Sci.* **2012**, *5*, 9107−9120.
(55) Myers, A. L.; Prausnitz, J. M. Thermodynamics of mixed-gas adsorption. *AIChE J.* **1965**, *11*, 121−127.
(56) Bloch, E. D.; Queen, W. L.; Krishna, R.; Zadrozny, J. M.; Brown, C. M.; Long, J. R. Hydrocarbon Separations in a Metal-Organic Framework with Open Iron(II) Coordination Sites. *Science* **2012**, *335*, 1606−1610.
(57) Xiang, S. C.; Zhang, Z. J.; Zhao, C. G.; Hong, K. L.; Zhao, X. B.; Ding, D. R.; Xie, M. H.; Wu, C. D.; Das, M. C.; Gill, R.; Thomas, K. M.; Chen, B. L. Rationally tuned micropores within enantiopure metal-organic frameworks for highly selective separation of acetylene and ethylene. *Nat. Commun.* **2011**, *2*, 1−7.
(58) Yang, S. H.; Ramirez-Cuesta, A. J.; Newby, R.; Garcia-Sakai, V.; Manuel, P.; Callear, S. K.; Campbell, S. I.; Tang, C. C.; Schroder, M. Supramolecular binding and separation of hydrocarbons within a functionalized porous metal-organic framework. *Nat. Chem.* **2015**, *7*, 121−129.
(59) Lin, R. B.; Li, L. B.; Wu, H.; Arman, H.; Li, B.; Lin, R. G.; Zhou, W.; Chen, B. L. Optimized Separation of Acetylene from Carbon Dioxide and Ethylene in a Microporous Material. *J. Am. Chem. Soc.* **2017**, *139*, 8022−8028.

DOI: 10.1021/jacs.8b08174
J. Am. Chem. Soc. 2018, 140, 15724−15730